Resonant coherent excitation of hydrogen atoms during grazing scattering from a LiF(001) surface

C. Auth and H. Winter
Institut für Physik der Humboldt-Universität zu Berlin, Invalidenstraße 110, D-10115 Berlin, Germany
(Received 7 January 2000; published 16 June 2000)

Protons with energies in the keV domain are scattered from a clean and flat LiF(001) surface under a grazing angle of incidence. For specific projectile energies, the periodic Coulomb field owing to the point-charge lattice of the ionic crystal leads to the ''resonant coherent excitation'' (RCE) of the $n=1$ to the $n=2$ states. This excitation is probed in our experiments via the intensity of Lyman-α light, emitted in the radiative decay of the excited states, as a function of projectile energy and azimuthal orientation of the crystal surface. We find clear evidence for RCE with a good signal to background ratio that allows us to perform detailed studies on the position, width, and line shape of the resonance.

PACS number(s): 79.20.Rf, 34.50.Fa, 34.70.+e

I. INTRODUCTION

When fast atoms or ions traverse a crystal foil under channeling conditions, the periodic Coulomb field in the solid may induce electronic transitions in the projectile. Okorokov [1] predicted that such a periodic perturbation for a projectile atom, traveling with constant velocity v, gives rise to resonant excitation phenomena with enhanced transition probabilities, the so-called resonant coherent excitation (RCE). The first experimental test to show evidence for this process was performed by same author and co-workers [2]. He^+ ions with energies of about 500–600 keV were sent through a thin monocrystalline Ag foil along a low index axial channel, and, for given interatomic spacings d, the velocity of the ions was chosen in a way that the resulting frequency of the periodic field $\nu=v/d$ matched the $n=1-n=4$ transition in the He^+ ion, i.e., a hydrogenlike atom. The excitation of the upper level was monitored by light in the visible spectral range emitted in the $n=4-n=3$, $\lambda=468$-nm transition. Indeed, in these early experiments, a weak resonance signal, i.e., an enhanced light intensity at about the expected ion velocity, was observed.

Closer inspection of the data, however, shows that the small width of the observed resonance signal can hardly be understood by a coherent process, since an unrealistically large coherence length (time) has to be assumed. This feature is contrasted by ''geometrical extensions'' of the excited He^+ $n=4$ states, which clearly exceed the dimensions of axial or planar channels within a Ag crystal, so that excited atoms will hardly survive a passage of several lattice sites within a crystal. Subsequent similar experiments on this problem by other groups were not conclusive and failed to show evidence for RCE phenomena [3–5].

A breakthrough in studies on RCE was achieved by Datz and co-workers [6–11], who made use of multicharged hydrogenlike and heliumlike ions. The binding energies of ground and first excited states for those ions are much larger than for neutral or singly charged ions (the binding energy of $1s$ level for N^{6+} ions is $E_B=7^2/2$ a.u.$=666.6$ eV), so that ground-state electrons bound to the projectile can survive the large impact-parameter collisions with lattice atoms under channeling (''frozen charge states''). RCE is monitored then by enhanced ionization cross sections for ions in excited states having lower binding energies and thus more extended spatial electronic distributions. The high energies for resonance transitions in multicharged ions makes it necessary to have considerable projectile velocities in order to induce RCE. As a consequence, those studies have to be performed—even by making use of higher-order harmonics—in the MeV energy range. Over the last two decades, detailed studies on RCE of multicharged ions in thin Au and Ag crystals have been performed by the Oak Ridge group [11–14]. A striking recent development in this respect is a study on hydrogenlike Ar^{17+} ions by Azuma *et al.* [15]. By making use of very high projectile energies of about 15 GeV, RCE of the resonance transition is induced in first order, and pronounced signals in the charge fractions are observed for the tuning of the azimuthal angle under planar channeling.

For surface channeling (''semiplanar channeling''), Kupfer and co-workers [16,17] pointed out that the screened potentials of lattice atoms of a metal lead to periodic electric fields in front of the solid, which can induce RCE in scattered projectiles. In a manner similar to that for foil transmission experiments, early attempts to observe RCE in surface scattering via optical transitions in He^+ ions failed [18]. However, recently Kimura *et al.* [19] scattered multicharged B ions with energies of about 5 MeV from a SnTe(100) surface under a grazing angle of incidence $\Phi_{in}\approx 0.3°$. RCE was detected via measurements of the B^{4+}/B^{5+} charge ratio showing a dip structure at about 5.85 MeV. This structure was attributed to the excitation of $n=2$ in hydrogenlike B^{4+} ions via the second-order harmonic of the periodic fields in front of the surface plane. In experiments with 23-MeV $^{15}N^{6+}$ ions scattered from a Pt(111) surface, Hatke *et al.* [20] observed, for a small angle of incidence, an enhancement of the mean charge state of scattered projectiles and interpreted their finding in terms of RCE. In a series of theoretical papers, Garcia de Abajo *et al.* [21–23] studied the emission of electrons induced by resonant coherent excitation and ionization processes. Specific spectral features and angular distributions for ejected electrons are predicted;

however, to our knowledge, no conclusive experimental studies on emitted electrons have been reported so far.

In this paper, we will describe work on a different aspect of RCE, i.e., the excitation of atoms during scattering from an *insulator surface*. In recent experiments with a LiF(001) surface, we showed that the *point-charge lattice* and the *band gap* of an ionic crystal give rise to various features that allow one to study RCE phenomena in a regime not accessible so far in previous studies [24]. We report on RCE studies with a neutral atom having a much smaller binding energy than multicharged ions, which can consequently be performed at projectile energies in the keV domain. The main issue of this paper will be a detailed investigation of RCE of the $n=1-n=2$ transition, induced in fast hydrogen atoms scattered from a clean and flat LiF(001) surface under a grazing angle of incidence. RCE is monitored here by means of Lyman-α light emitted in the radiative decay of $n=2$ states as a function of the projectile energy (velocity) and azimuthal orientation of the crystal surface. We will show that the good signal-to-noise ratio of the data allows us to perform a detailed analysis on the position, splitting, and width of the resonance signals. In photon-particle coincidence measurements, we obtained reduced background signals and an estimate on excitation probabilities.

II. POTENTIALS AND ELECTRIC FIELDS IN FRONT OF THE SURFACE OF AN IONIC CRYSTAL

The potential in front of the surface of an ionic crystal is composed of two different contributions: (i) the screened potential owing to the cores of lattice atoms, and (ii) the unscreened Coulomb potential of a point-charge lattice with charges $\pm e$ owing to the ionic bonds. Potentials of type (i) have been made use of in studies on RCE so far, performed with metal or semiconductor targets. One of the alternative aspects of our work is the dominant role of potentials of type (ii) concerning the RCE process. In the following, we will show that the latter potentials have a defined periodic structure, where fundamental modes completely dominate any overtones.

For a point-charge representation of the crystal lattice with charges $\pm e=\pm 1$ a.u., the potential in front of the surface plane ($z>0$) is given by [16,24]

$$V(\vec{r})=\sum_{\substack{m,k \\ m+k=\text{even}}} V_{mk}(z)\cos(mgx)\cos(kgy), \qquad (1)$$

with the reciprocal lattice constant $g=2\pi/d$, $d=7.6$ a.u. being the spacing between lattice sites of the same charge; x and y are directed along orthogonal low index directions in the surface plane, and

$$V_{mk}(z)=\frac{16}{d}(m^2+k^2)^{-1/2}\frac{\exp\{-g(m^2+k^2)^{1/2}z\}}{1+\exp\{-\pi(m^2+k^2)^{1/2}\}}, \quad (2)$$

where m and k denote the orders of harmonics with the selection rule $m+k=$ ''even.'' From Eq. (2) follows an exponential damping of the potential amplitudes in Eq. (1) with a pronounced dependence on m and k. Consequently, fundamental frequencies ($m=k=1$) completely dominate the periodicities. This is different from previous experiments, where potentials owing to screened atomic cores in metals are used, resulting in substantial contributions of higher-order harmonics. In almost all studies so far, RCE has been induced by overtones in order to reduce projectile energies. Figure 1 shows coefficients $V_{mk}(z)$ for the first few harmonics as a function of the distance from the surface z. The larger decay constants in the exponent of Eq. (2) for increasing m, k result in a dominant fundamental mode in the periodic potential structures. For distances of about 3–4 a.u., relevant for RCE in our studies on H $n=2$, the fundamental ($m=1$, $k=1$) mode exceeds contributions of higher-order harmonics by more than one order of magnitude. Thus we expect that in studies using the surface of an ionic crystal there will be period potentials (electric fields), which are free from overtones.

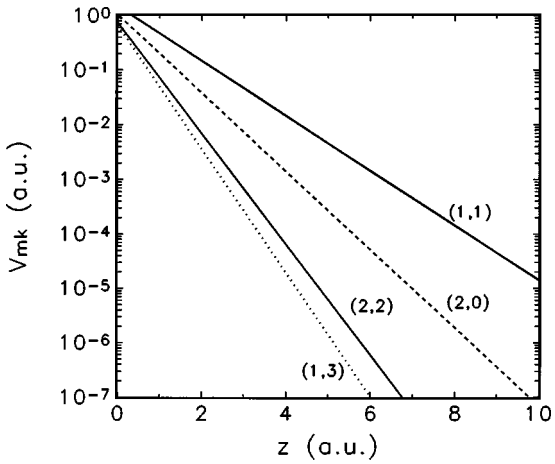

FIG. 1. Coefficients V_{mk} as a function of distance z from the surface plane.

A second important feature of the periodic potential structure for a planar arrangement of lattice sites can also be derived from Eq. (1). For grazing surface scattering, i.e., planar channeling [25] from the topmost layer of surface atoms, the motion of projectiles proceeds within a scattering plane defined by the direction of the incident beam and the surface normal. Energies for the motion normal and parallel with respect to the surface plane are conserved (small energy loss of projectiles neglected). Projections of trajectories into the surface plane (xy plane) along a direction x' are given by the simple relations $x=\cos\theta x'$ and $y=\sin\theta x'$. θ denotes the azimuthal angle to the x axis, which is chosen here along the low index $\langle 100\rangle$ direction of the crystal lattice. Then Eq. (1) can be written as

$$V(\vec{r})=V_{11}(z)\{\cos[g(\cos\theta-\sin\theta)x] + \cos[g(\cos\theta+\sin\theta)x]\}/2. \qquad (3)$$

For an azimuthal detuning from $x(\theta\neq 0)$, the modulation in the periodic potential leads to the generation of sidebands $g(\cos\theta\pm\sin\theta)$. This characteristic splitting of the periodicity in the potential for an azimuthal detuning under planar chan-

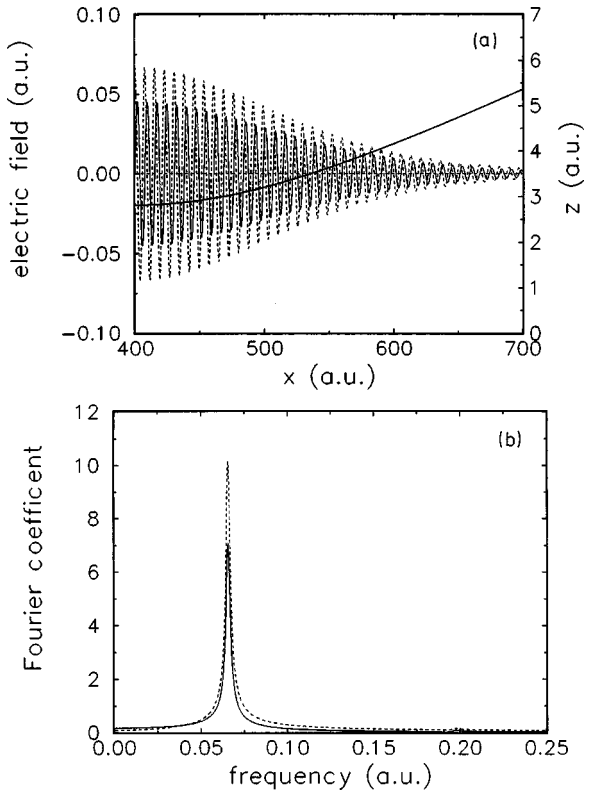

FIG. 2. (a) Plots of the electric-field components E_x (dashed curve) and E_z (solid curve) for an H atom scattered in front of a LiF(001) surface under a grazing angle of incidence with velocity $v=0.5$ a.u. The thick solid curve represents the outgoing trajectory. The projectiles are scattered along $\langle 100\rangle$ on top of a string of surface atoms. (b) Fourier coefficients for E_x and E_z shown in (a).

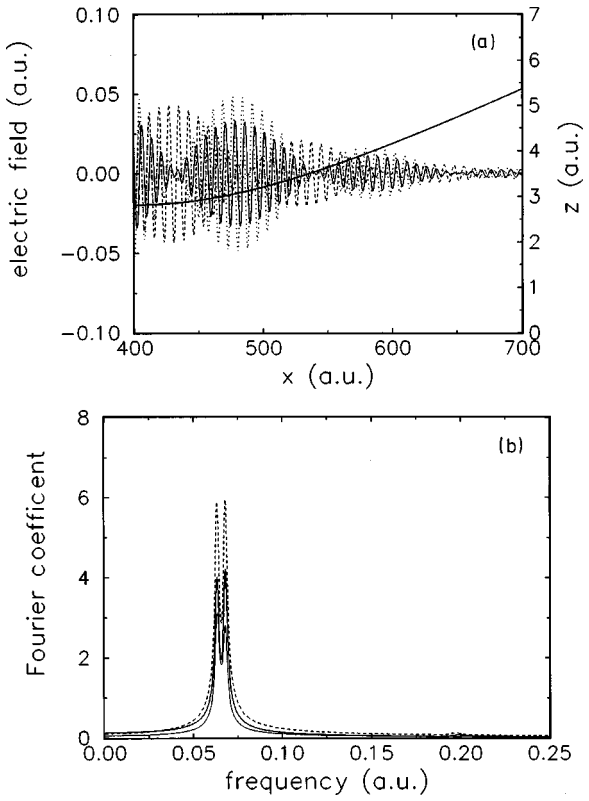

FIG. 3. (a) Same as Fig. 2(a), but for a trajectory with an azimuthal detuning of $\theta=2°$ with respect to $\langle 100\rangle$. E_y (dotted curve). (b) Fourier coefficients for E_x (dashed curve), E_y (thin solid curve), and E_z (thick solid curve) shown in (a).

neling is an important criterion to demonstrate evidence for RCE in experimental investigations.

The resulting frequency owing to the periodic potential equals an electronic excitation energy in the atom ε at an atomic projectile velocity $v_{\rm res}=\varepsilon/g(\cos\theta\pm\sin\theta)$. Then for a projectile of mass M, the projectile energy resonance condition for planar channeling is given by

$$E_{\rm res}=\tfrac{1}{2}Mv_{\rm res}^2=\frac{1}{8\pi^2}\frac{d^2M\varepsilon^2}{(\cos\theta\pm\sin\theta)^2}, \tag{4}$$

where the ''$\pm$'' sign in Eq. (4) denotes a splitting of the resonance into two sidebands for $\theta\neq 0$. For our studies on H $n=2$ we have $\varepsilon=10.2\,\text{eV}=3/8$ a.u. and $M=M_{\rm H}=1836$ a.u., so Eq. (4) reads $E_{\rm res}=5.14\,\text{keV}/(\cos\theta\pm\sin\theta)^2$. This means that studies on RCE can be performed in the domain of keV energies, i.e., by making use of a small ion accelerator or even ion source instead of large accelerator facilities providing heavy ion beams in the MeV or even GeV domain.

In order to summarize the discussion in this section, we illustrate in Fig. 2(a) the electric-field components E_x, E_y, and E_z for a trajectory of 6-keV H atoms scattered under $\Phi_{\rm in}=0.75°$ from LiF(001) along $\langle 100\rangle$, i.e., $\theta=0°$ and $y=0$. The data show for E_x and E_z (E_y vanishes in this case) a damped oscillatory structure with a defined phase shift between the two field components of $\pi/2$. The Fourier transform of this field structure [Fig. 2(b)] for the outgoing trajectory and $z\geqslant 3$ a.u. reveals a well defined peak at the fundamental frequency, well approximated by a Lorentzian line shape. Note that higher-order harmonics can hardly be identified in the spectrum.

Figure 3(a) shows the field components for the same conditions as in Fig. 2(a), but $\theta=2°$. Beating phenomena are clearly seen for all field components, which result for the Fourier spectra [Fig. 3(b)] in the expected splitting of the resonance into two sideband components.

III. EXPERIMENT

The concept of our experiments on the RCE of keV H atoms in front of a LiF(001) surface is outlined by the energy diagram in Fig. 4. LiF is a wide-band-gap insulator with a band gap of $E_g\approx 14$ eV, which extends to vacuum energies. The valence band is formed by F $2p$ electrons localized at F^- lattice sites of the crystal. The top of this flat band has a binding energy of 12 eV [24,25]. The energy of the atomic states is slightly shifted via image charge interaction in front of the surface. Impinging H^+ ions are efficiently neutralized via resonant neutralization by valence-band electrons. In case the resonance condition given in Eq. (4) is fulfilled, the $1s$ electron is ''pumped'' to an $n=2$ state via RCE owing to the periodic surface potential and the corresponding oscillations in the electric-field components.

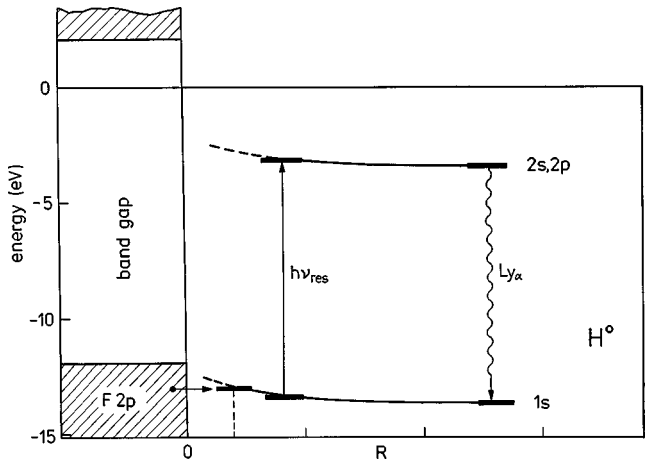

FIG. 4. Energy diagram to illustrate the electronic excitation of hydrogen atoms in front of a LiF surface and subsequent radiative decay.

At the distance of closest approach to the surface $z_{\min}$ of about 3 a.u. for the conditions of our experiments, the electron cloud of the 1*s* ground state is expected to be hardly affected by the presence of the solid. Furthermore, this state is basically stable against electron loss via resonant ionization, because the 1*s* level is in resonance with the fully occupied valence band. Owing to the band gap, electron loss means promotion to vacuum energies.

For excited $n=2$ states, the electronic distributions are characterized by larger radii so that, at distances around $z_{\min}$ a substantial overlap with the solid is expected. As a consequence, the lifetimes of excited states will be strongly reduced by presumably binary collision types of interaction mechanisms (electron promotion by formation of molecular orbitals, etc.). At somewhat larger distances on the outgoing trajectory, the overlap with the solid and the effects on the lifetimes of excited states will be reduced. For those distances the wide band gap of the insulator is important, since the presence of the electronic gap suppresses resonant electronic transitions between the excited atom and the solid. So excited states can survive from the interaction with the solid surface on the receding part of the projectile trajectory. This important feature, which favors the observation of RCE for weakly bound electronic levels in neutral atoms, is absent in front of metal surfaces, where atomic states with binding energies smaller than the work function of metals (typically 5 eV) are efficiently quenched via long-range resonant ionization.

Excited atoms, which survive from the interaction with the surface, decay via the emission of a Lyman-α photon ($\lambda=121.6\,\mathrm{nm}$) to the ground state with a mean lifetime $\tau=1.6\,\mathrm{ns}$. Detection of these photons will monitor the RCE process in our experiments. In this respect, our scheme of radiative detection is equivalent to those few studies with MeV multicharged ions, where RCE is investigated via x-ray emission [12,26].

In our experiments, a well collimated beam of H^+ ions with energies ranging from 2 to 12 keV is scattered under grazing angles of incidence $\Phi_{\mathrm{in}}=0.25°$ to 3° from a clean and flat LiF(001) surface. In order to avoid a macroscopic

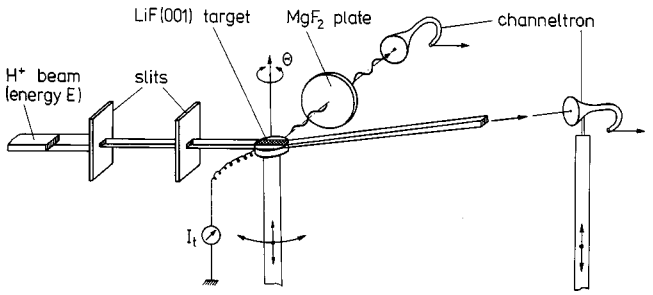

FIG. 5. Sketch of the experimental setup.

charging up of the insulator by incident ions, the target is kept at a temperature of about 300 °C, where LiF shows sufficient conductivity [27]. The target is mounted on a precision manipulator in an UHV chamber at a base pressure of about 10^{-10} mbar. The preparation of the target is achieved by cleaving and mechanical polishing in air, and then by many cycles of grazing sputtering with 25-keV Ar^+ ions at $\Phi_{\mathrm{in}}\approx 2°$ to 3° at 300 °C and subsequent annealing up to temperatures of about 400 °C under UHV conditions. During sputtering, an azimuthal rotation of the target is performed, where the uncompensated target current shows sharp peaks for incidence along low index directions in the surface plane, in particular ⟨100⟩. This enhancement in kinetic electron emission is used for precise *in situ* azimuthal settings of the crystal surface. In the final state of preparation of the target surface, well defined angular distributions for scattered projectiles are recorded, which serve as an indication for a target surface with a low density of steps (mean terrace width about 100 nm). Details on this subject are reported elsewhere [28].

Figure 5 shows a sketch of the experimental setup. The Lyman-α light is detected normal to the plane of scattering by means of a channeltron (VALVO X919 BL) with a quantum efficiency of $\varepsilon_{\mathrm{det}}\approx 2$–4 %. This detector is sensitive to electromagnetic radiation with wavelengths smaller than about $\lambda_d=150\,\mathrm{nm}$. The effective solid angle for detection is estimated to be $\Omega_{\mathrm{det}}=0.08\times 4\pi$. In front of the channeltron a thin MgF_2 plate with a cutoff wavelength $\lambda_{\mathrm{co}}=115\,\mathrm{nm}$ is mounted. The transmission for Lyman-α light is $T_{\mathrm{MgF}}\approx 0.5$. Within the spectral range $\lambda_{\mathrm{co}}\leqslant\lambda\leqslant\lambda_d$, our device for detection will record only Lyman-α radiation from the line spectra of hydrogen atoms. However, we note that this setup will not discriminate against light within the above wavelength limits, which stems from sources other than inneratomic transitions.

In the measurements, RCE resonances are tuned by scanning either the projectile energy or the azimuthal angle [see also Eq. (4)]. We primarily concentrated on a variation of the projectile energy, where the data are normalized to the intensity of scattered projectiles, recorded by means of a second channeltron with a 0.5-mm aperture. The scanning of the projectile energy was achieved by a voltage applied to an insulated platform, on which a 10-GHz ECR ion source with extraction electrode, beam transport, and analyzing magnet is mounted.

IV. RESULTS AND DISCUSSION

In our first experiment we oriented the ⟨100⟩ direction in the target surface parallel with respect to the axis of the

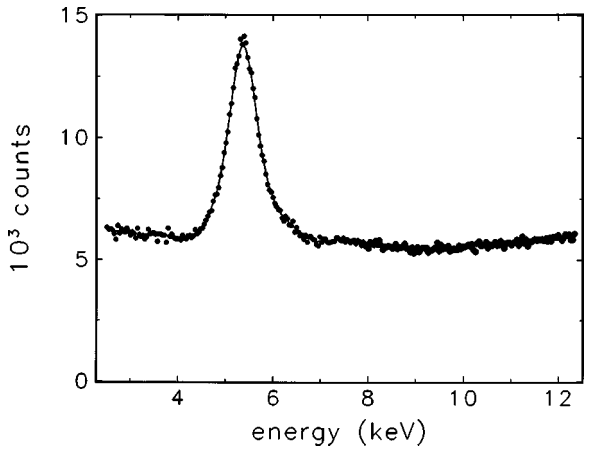

FIG. 6. Normalized counts of the Lyman-α detector as a function of projectile energy for the scattering of H^+ ions from a LiF(001) surface under $\Phi_{in}=0.75°$. The solid line is drawn to guide the eyes.

incoming H^+ beam ($\theta=0°$), and recorded the normalized Lyman-α intensity as a function of projectile energy from 2.5 keV to 12 keV. The focusing elements of the accelerator were adjusted in a way that the overall variation of the beam intensity during an energy scan was not too large; i.e., the monotonic increase with energy did not in general exceed about 50%. In Fig. 6 we show a plot of the normalized counts over projectile energy. The data reveal a clear resonance structure superimposed on a constant background signal of about 50% from the counts obtained in resonance. Closer inspection of the resonance position shows that E_{res} is shifted from 5.14 keV, derived from Eq. (4), by about 250 eV toward larger energies. This shift is owing to projectile energy loss during surface scattering and will be discussed in detail below. At about 7.5 keV the measurement might indicate a further resonance signal owing to the RCE of $n=3$ ($E_{res}=7.22$ keV), which is monitored here via partial cascading to $n=2$; however, the signal to background ratio is too poor for an analysis of data. We will concentrate here on the RCE of $n=2$.

We performed a controlled variation of the azimuthal angle θ under otherwise unchanged conditions. In Fig. 7 we display data for $\theta=0°$, 3°, 5°, and 7°. The data clearly show the splitting of the resonance as expected from Eq. (4). For a quantitative comparison with the theoretical predictions, we have plotted in Fig. 8 the resonance energies deduced from the maxima of data shown in Fig. 7 as a function of the azimuthal detuning from ⟨100⟩. The agreement between experimental and theoretical resonance energies (solid curves) is fairly good; in particular, the splitting of the resonance is reproduced on a quantitative level. Closer inspection of the data reveals a slight shift of the experimental resonance toward larger projectile energies.

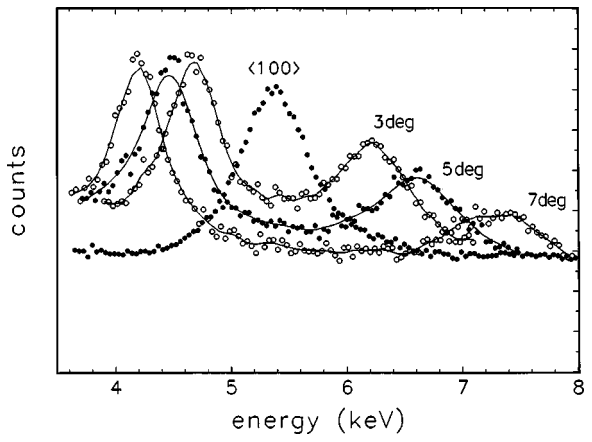

FIG. 7. Same as Fig. 6, but for $\theta=0°$ (⟨100⟩), 3°, 5°, and 7°. The solid lines are drawn to guide the eyes.

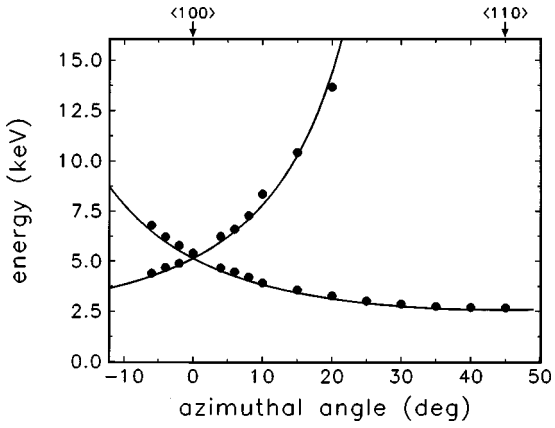

FIG. 8. Experimental resonance energy for the RCE of $n=2$ in hydrogen atoms in front of a LiF(001) surface as function of the azimuthal angle. The solid curves represent the resonance conditions given by Eq. (4).

In order to investigate this shift in energy of the resonance, we recorded by means of an electrostatic analyzer with cylindrical electrodes of 0.5-m radius (energy resolution $\delta E/E<10^{-3}$) energy spectra for scattered H^+ beams. As a representative example we show in Fig. 9 spectra for 5.5-keV H^+ ions scattered specularly with $\Phi_{in}\approx 1°$ and $\theta=0°$ (⟨100⟩) as well as a high index direction (''random'') from the LiF(001) target. The energy spectra show peaks at an energy loss of about 300–310 eV and differ only slightly in

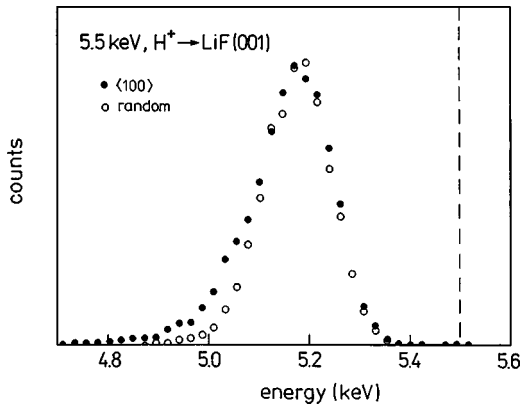

FIG. 9. Energy spectra for 5.5-keV H^+ ions scattered under $\Phi_{in}\approx 1°$ from a LiF(001) surface along ⟨100⟩ (full circles) and under a ''random'' direction (open circles). The dashed line indicates the energy of the incident projectiles.

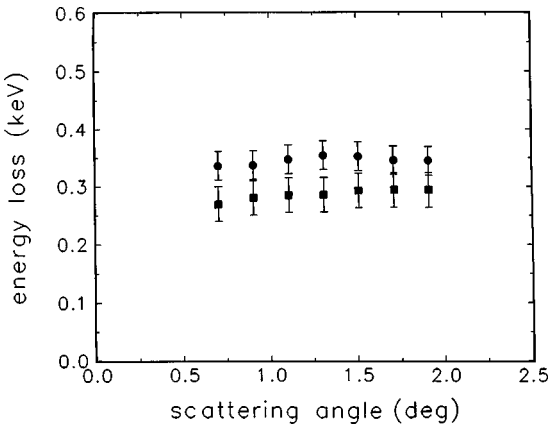

FIG. 10. Energy loss as a function of scattering angle for 5.4-keV (full squares) and 6.0-keV (full circles) H^+ ions scattered from a LiF(001) surface.

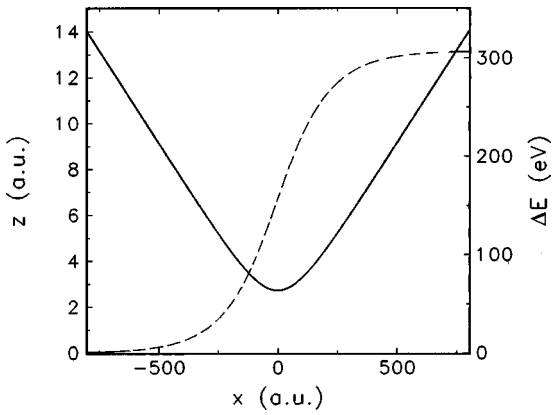

FIG. 11. Trajectory (thick solid curve) and accumulated energy loss for 5.5 keV H^+ ions scattered from a LiF(001) surface. For details see text.

the low-energy tails for the two azimuthal settings. The full width at half maximum (FWHM) amounts to about 160–170 eV. In similar measurements we have studied the mean energy loss as a function of the angle of incidence and scattering. In Fig. 10 we present corresponding data obtained at 5.4 and 6 keV. We find that the mean energy loss is constant for a variation of the angle of scattering (incidence).

Kimura *et al.* [29,30] have shown that from the angular dependence of the energy loss for grazing, ion surface collisions, position-dependent stopping powers $-dE/dx(z)$ can be derived. The corresponding analysis of data is particularly simple for cases where the energy loss is constant with the angle, as observed here. Then for a collective planar interaction potential $U(z)=a_1\exp(-a_2 z)$, the position-dependent stopping power is $-dE/dx(z)=-dE/dx(0)\exp(-a_2 z/2)$, with $-dE/dx(0)=\Delta E(a_2/2\pi)(a_1/E_0)^{1/2}$. From a fit to a planar potential derived from universal interatomic potentials (Ziegler-Biersack-Littmark) [31] for the two sublattices, i.e., H-Li and H-F, we deduce $a_1=13.9$ eV and $a_2=0.88$ a.u.$^{-1}$. From the measured energy loss $\Delta E=310$ eV at an energy $E_0=5.4$ keV we obtain the position-dependent stopping power $-dE/dx(z)=2.1$ eV/a.u. $\exp(-0.44z/\text{a.u.})$.

Based on this stopping power we summed up the energy loss over a typical trajectory for our studies. Figure 11 shows trajectory and accumulated energy loss for 5.4-keV H^+ ions scattered from LiF(001) under $\Phi_{in}=0.75°$ (note that this angle is increased by image charge interaction on the incident path to $\Phi_{in}^{im}=0.92°$). The energy loss (dashed curve) grows with trajectory length and has the largest increase around the apex. In our measurements on RCE we found that the peak position of the resonance for $\theta=0°$ is shifted from the expected value by about 250–260 eV. From the energy loss as given in Fig. 11, we conclude that this loss is accumulated when the projectile has reached a distance of about 3.5–4 a.u. on the receding part of the trajectory. This finding is interpreted in terms of the simple picture that at closer distances the overlap of the electronic cloud for the excited level is too pronounced, and an efficient quenching is expected. In passing we note that the mean radius for the $2p$ state of an unperturbed hydrogen atom is $\langle r\rangle_{2p}=5$ a.u. Furthermore, we point out that beyond those distances of survival of the excited levels the band gap of the insulator plays an essential role, since reionization of those levels via resonant tunneling is suppressed. This is considered to be in clear contrast to metal targets, where resonant transfer into unoccupied metal states leads to an efficient ionization of the excited $n=2$ level up to distances $z\approx 10$ a.u., and the observation of RCE phenomena becomes extremely unlikely then.

Aside from the position, the width of the observed RCE resonance is an important quantity. In this respect it is of particular interest to identify the dominant contributions to the broadening of the resonance curves observed here. In Fig. 12 we have plotted the FWHM of resonance curves (see, e.g., Fig. 6) as a function of the angle of incidence (open circles). Since in these studies H^+ projectiles are used, the angle is enhanced by image charge forces. In an additional experimental study we observed an energy gain $E_{im}\approx 0.5$ eV owing to the image potential for H^+ ions in front of a LiF(001) surface. The image effects are stopped by the neutralization of the projectiles at about 3–4 a.u. on the in-

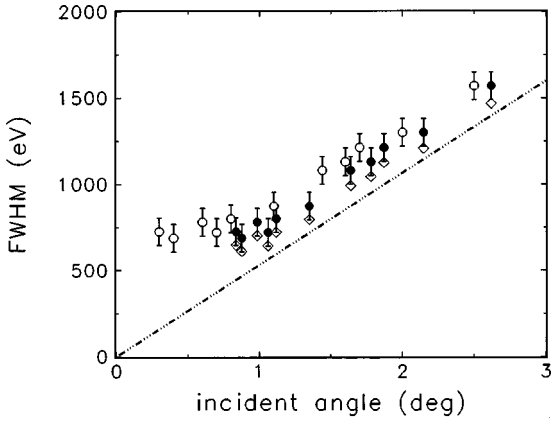

FIG. 12. FWHM of the RCE resonance as a function of the angle of incidence (open circles). Full circles represent the data corrected for image charge effects on the trajectories, open diamonds show data after deconvolution with energy distribution for the scattered beam. The line represents calculations of the width by integration of the Schrödinger equation for this problem on the outgoing trajectory starting at $z=3.5$ a.u.

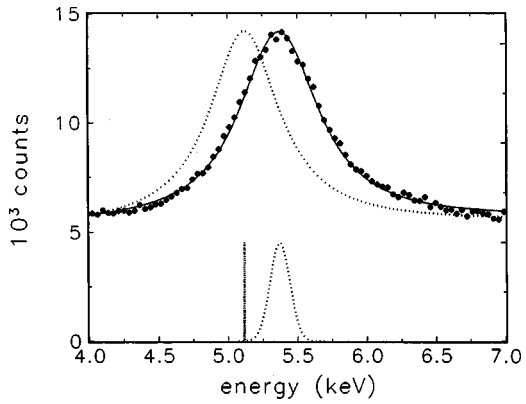

FIG. 13. Same data as shown in Fig. 6 fitted by a Lorentzian line shape under convolution of energy loss and straggling (bottom of figure) for the scattered beam.

cident part of the trajectories. The image charge attraction enhances the effective angle of incidence according to $\Phi_{\mathrm{in}}^{+}=(\Phi_{\mathrm{im}}^2+E_{\mathrm{im}}/E_0)^{1/2}$ [32]. The full circles in Fig. 12 represent data corrected accordingly. The corrected data reveal a linear dependence of the width on angle. We compare the data with calculations based on the solution of the time-dependent Schrödinger equation for a five-state basis set of the electronic structure of the atom, perturbed by the periodic Coulomb field owing to the point charges of the crystal lattice [24,33]. In accordance with the analysis of the energy loss given above, the starting point of the integration is set to $z=3.5$ a.u. on the outgoing path. Details on the calculations will be given elsewhere [33]. The strict proportionality of the width with angle (or inverse of the interaction time) indicates that the interaction time is the dominant contribution to the broadening of the RCE signal. The experimental data show a constant offset from the theoretical dependence.

The origin for this offset can be understood to a major extent by the energy straggling of the projectiles during the scattering from the surface. From the spectra displayed in Fig. 9 we deduce for complete trajectories at 5.5 keV a straggling of $\delta E\approx 170$ eV. In a fitting procedure we assume a Lorentzian line shape for the RCE signal as function of energy

$$I(E)=\frac{A}{(E-E_{\mathrm{res}})^2+(\delta E_{\mathrm{res}}/2)^2}+B, \tag{5}$$

with A (amplitude), B (background), E_{res} (resonance energy), and δE_{res} (resonance width) being the fitting parameters. This dependence is convoluted with the energy loss and energy straggling effective for RCE as discussed above; i.e., loss and straggling amount to about 80% from the data for a full trajectory (see inset at bottom of figure). In addition, we assume that both quantities scale linearly with energy E [34]. The result of such a procedure of data handling is shown in Fig. 13 for measurements performed under $\Phi_{\mathrm{in}}=0.75°$ and $\theta=0°$. The solid curve represents a best fit to the data, whereas the dotted curve is the deconvoluted resonance signal as given by Eq. (5). From this analysis we conclude that the measured width of about 720 eV is reduced to $\delta E_{\mathrm{res}}=640$ eV, in case the effect of projectile energy dissipation during the scattering is eliminated. The corrected data still show a slight systematic shift from theory. This shift might be explained by an unresolved Stark splitting owing to the field by screened atomic cores (not considered in theory), by a broadening of the resonances by a slight mistuning of θ from $\langle 100\rangle$, or by the slight angular divergence of the scattered beam. In view of the uncertainties in the measurements and analysis of data, we are not able to clear up this item. So we conclude that the observed widths of RCE data are dominated by broadening owing to the interaction time with the periodic field structure. Energy straggling of the projectile beam slightly increases the width, and energy loss shifts observed resonance energies to higher energies.

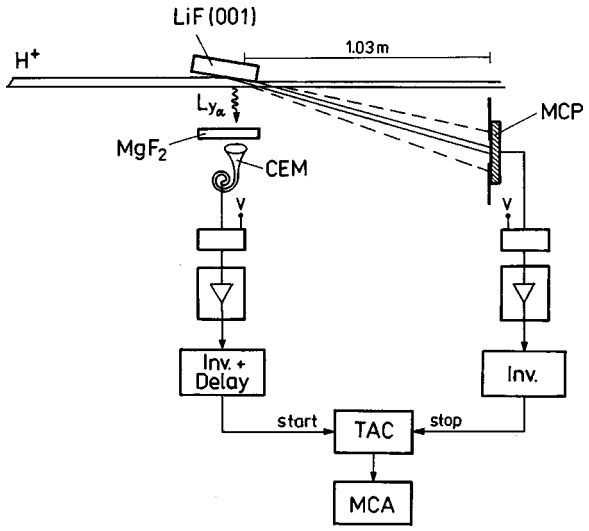

FIG. 14. Sketch of the experimental setup for the photon-particle coincidence studies.

V. PHOTON-PROJECTILE COINCIDENCES

In the second part of our investigations on the RCE of hydrogen atoms, we studied the emission of Lyman-α photons in coincidence with scattered projectiles. The setup is sketched in Fig. 14. An important modification in comparison to the work outlined above is the detection of projectiles by means of a multichannel plate (MCP). Owing to the larger acceptance angle, the efficiency of the MCP for detecting scattered projectiles is much higher than the channeltron detector. The coincidence spectra are recorded with standard nuclear electronics and a multichannel analyzer (MCA). Pulses from the photon branch provide the start signal for the time-to-amplituder converter (TAC), pulses from the MCP the stop signal. Typical counting rates amount to about 5 counts/s for the start and about 40 000 counts/s for the stop channel.

Two typical coincidence spectra are displayed in Fig. 15, recorded at an energy of $E=5.4$ keV, i.e., at the maximum of the RCE probability, and at $E=7.5$ keV, i.e., off-resonance. The data show spectra as a function of the start-stop time interval with well defined true coincidences on top of a low random background. The different peak heights for the true

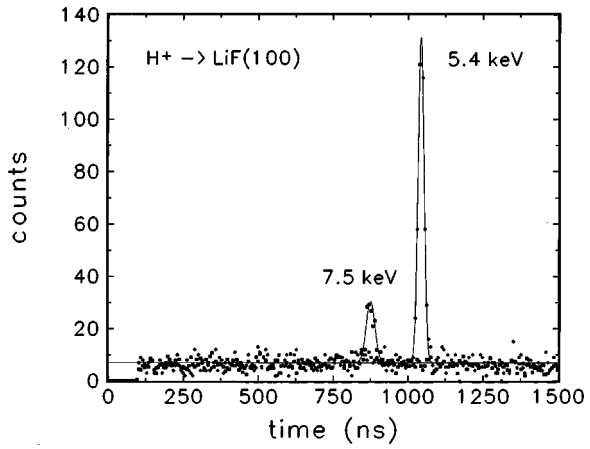

FIG. 15. TAC spectra obtained for 5.4-keV (dots) and 7.5-keV (squares) H^+ ions scattered from a LiF(001) surface under $\Phi_{in} \approx 1°$. The flight time for the distance of 1.03 m from the target to the MCP is about 1 μs.

coincidences reveal the resonance of the excitation with projectile energy. The data are analyzed by summing up the true coincidences (background owing to random coincidences is substracted) and by normalization to the total number of counts in the stop channel. A typical time for recording a spectrum amounts to about 1 to 2 h. A plot of the normalized coincidences versus projectile energy is given in Fig. 16. The data show a pronounced resonance signal with the maximum at $E=5.4$ keV, the resonance energy for RCE as outlined in the previous section. A striking result of the data is a clearly improved signal to background ratio in comparison to data without coincidence (as, e.g., shown in Fig. 6) from a factor of about 2 to about 6. The solid curve is a best fit to a Lorentzian line shape comprising a background with a slight linear increase with energy. Different types of symbols represent runs taken at different days.

From the observed enhanced RCE signal to background ratio for specularly reflected projectiles we conclude that a

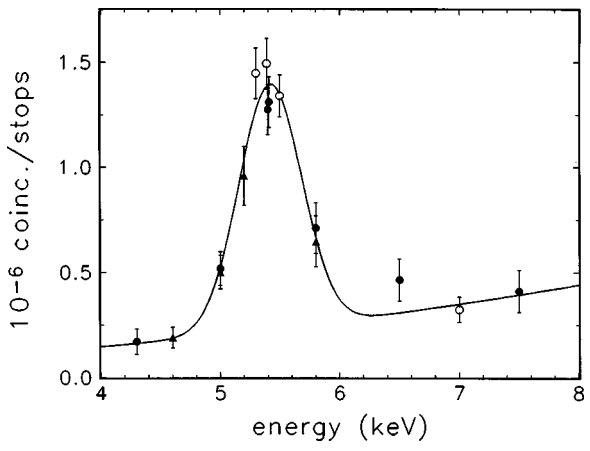

FIG. 16. Ratio of the number of true coincidences to stop counts as a function of projectile energy derived from spectra as displayed in Fig. 15. The solid line represents a best fit to the data by a Lorentzian line shape with an energy-dependent background. Different symbols represent data taken on different days.

substantial fraction of the nonresonant background is owing to scattering events with larger angular deflections. We ascribe the origin of these events to binary types of collisions of projectiles with atoms forming defect structures, primarily steps, at the target surface. In previous studies with metal surfaces it has been shown that those collisions lead to efficient populations of excited atomic levels in grazing ion surface scattering [35]. The nonresonant background in the coincidence data (Figs. 15 and 16) might be caused by electron capture assisted by kinematic effects (''parallel velocity effect'' [36,37]), which reduce the energy defect between the valence band and the excited $n=2$ level. This interpretation is supported by the observation that a small fraction of H^+ ions (about 1%) is found in the scattered beam that increases with energy [38].

The probability for the RCE of $n=2$ in scattered H atoms P_γ is deduced from the rate of true coincidences n_T, which is simply related to the counting rate for the stop channel (particles) n_p according to $n_T=\varepsilon_\gamma n_p$, with ε_γ being the total detection efficiency of the photon branch $\varepsilon_\gamma = P_\gamma \varepsilon_{\rm det} T_{\rm MgF_2} \Omega_{\rm det}/4\pi$. For a fixed time $\Delta t \approx 90$ min we measured $N_T = n_T \times \Delta t = 583$ and $N_p = n_p \times \Delta t = 1.95 \times 10^8$ and obtained

$$P_\gamma = \frac{N_T}{N_p \varepsilon_{\rm CEM} T_{\rm MgF_2} \Omega_{\rm det}/4\pi} = 2.4 \times 10^{-3} \qquad (6)$$

as the probability for the RCE of $n=2$. Since the detection efficiency of the channeltron for Lyman-α radiation is known with large uncertainty only (from handbook data we derive $\varepsilon_{\rm det} \approx 0.03 \pm 0.01$), we estimate the uncertainty of P_γ to be about 50% of the above value.

In these experiments, the counting rates for the start and stop channels amount to $n_\gamma \approx 4.3$ count/s and $n_p = 40\,600$ count/s. From the ratio $n_\gamma/n_p = \varepsilon_\gamma/\varepsilon_p$ we find for the noncoincident excitation probability

$$P_\gamma^{\rm nc} = \frac{f_p \varepsilon_{\rm MCP} n_\gamma}{\varepsilon_{\rm det} T_{\rm MgF_2} n_p \Omega_{\rm det}/4\pi} = 1.4 \times 10^{-2}, \qquad (7)$$

where $f_p = 0.4$ is the fraction of projectiles scattered within the sensitive area of the MCP detector and $\varepsilon_{\rm MCP} = 0.4$, the detection efficiency of the MCP for atoms with keV energies. In the resonance curves (see, e.g., Fig. 6), a background of about 50% is observed so that we conclude from $P_\gamma^{\rm nc}$ a total RCE probability for the scattered beam of 7×10^{-3}. This is clearly larger than P_γ evaluated from the coincidence data and reflects the error in the present analysis of data owing to uncertainties in the detection efficiencies, etc. For a more accurate analysis in this respect, a careful calibration of the photon and particle detection branch has to be performed. Such a procedure is beyond the scope of the present work.

For comparison of our experimental RCE probabilities with theory, no calculations are known to us. Finding a solution of the time-dependent Schrödinger equation for a hydrogen atom moving in front of a point-charge lattice is a feasible task [33]; however, as pointed out above, the fraction of atoms that emit photons after RCE have survived

from subsequent electron loss. Since the loss mechanism plays an essential role for the final occupation of $n=2$ in scattered atoms, an appropriate modeling of the loss mechanism is important for a quantitative description of excitation probabilities. In recent studies on charge fractions as a function of projectile energy [38], we observed the RCE resonance via enhanced H^+ fractions in H beams scattered from LiF. These enhanced fractions are ascribed to a quenching of excited ($n=2$, and higher n) levels after RCE. About 1% of all scattered projectiles are found to have undergone such an excitation and ionization cycle at projectile energies around 5 keV.

VI. CONCLUSION

In conclusion, by scattering keV-H^+ ions from a LiF(001) under a grazing angle of incidence we found clear evidence for the RCE of the $n=2$ level in fast hydrogen atoms moving in front of the periodic point-charge lattice of an ionic crystal. For the survival of excited atoms the wide band gap of the insulator plays an essential role, since this gap suppresses the reionization of excited levels via resonant tunneling into the solid. As a consequence, RCE is observed for weakly bound electronic states in a neutral atom with an excellent signal to background ratio. The good quality of the resonance signals allows us to study in detail resonance positions, widths, and excitation probabilities. It turns out that the resonance energies are shifted due to energy loss for projectiles during the scattering. The resonance widths are primarily given by transit-time broadening and, to a lesser extent, by the energy straggling of the scattered beam. Since it is feasible to analyze the polarization of Lyman-α light [39], it would be an interesting future project to study the polarized light emission after RCE. Such a study might provide information on the production of coherent atomic states of opposite parity within a manifold. Such a coherent superposition of excited atomic states (''*sp* coherence'') is a well established feature in beam-foil spectroscopy [40] and atomic collision physics [41].

ACKNOWLEDGMENTS

The assistance of Dr. A. Mertens, K. Maass, and R.-A. Noack in running the experiments is gratefully acknowledged. We acknowledge fruitful discussions with Dr. A. G. Borisov (Orsay), Professor J. P. Gauyacq (Orsay), and Dr. J. F. Garcia de Abajo (San Sebastian). This work was supported by the Deutsche Forschungsgemeinschaft (DFG) under Contract No. Wi 1336.

[1] V. V. Okorokov, Pis'ma Zh. Eksp. Teor. Fiz. **2**, 175 (1965) [JETP Lett. **2**, 111 (1965)].
[2] V. V. Okorokov, D. L. Tolchenkov, I. S. Khizhnyakov, Y. u. N. Chlebukov, and Yu. Ya. Lapitsky, Phys. Lett. **43A**, 485 (1973).
[3] M. J. Gaillard, J. C. Poizat, J. Remillieux, and M. L. Gaillard, Phys. Lett. **45A**, 306 (1973).
[4] H. G. Berry, D. S. Gemmell, R. E. Holland, J. C. Poizat, J. Remillieux, and J. N. Worthington, Phys. Lett. **49A**, 123 (1974).
[5] M. Mannami, H. Kudo, M. Matsushita, and K. Ishii, Phys. Lett. **64A**, 136 (1977).
[6] S. Datz, C. D. Moak, O. H. Crawford, H. F. Krause, P. F. Dittner, J. Gomez del Campo, J. A. Biggerstaff, P. D. Miller, P. Hvelplund, and H. Knudsen, Phys. Rev. Lett. **40**, 843 (1978).
[7] S. Datz, J. Phys. (France) **40**, C1 (1979).
[8] C. D. Moak, J. A. Biggerstaff, O. H. Crawford, P. F. Dittner, S. Datz, J. Gomez del Campo, P. Hvelplund, H. Knudsen, H. F. Krause, P. D. Miller, and S. H. Overbury, Nucl. Instrum. Methods Phys. Res. **194**, 327 (1982).
[9] O. H. Crawford and R. H. Ritchie, Phys. Rev. A **20**, 1848 (1979).
[10] C. D. Moak, S. Datz, O. H. Crawford, H. F. Krause, P. F. Dittner, J. Gomez del Campo, J. A. Biggerstaff, P. D. Miller, P. Hvelplund, and H. Knudsen, Phys. Rev. A **19**, 977 (1979).
[11] P. D. Miller, H. F. Krause, J. A. Biggerstaff, O. H. Crawford, S. Datz, P. F. Dittner, J. Gomez del Campo, C. D. Moak, N. Neskovic, P. L. Pepmiller, and M. D. Brown, Nucl. Instrum. Methods Phys. Res. B **13**, 56 (1986).
[12] S. Datz, P. F. Dittner, H. F. Krause, C. R. Vane, O. H. Crawford, J. S. Forster, G. S. Ball, W. G. Davies, and J. S. Geiger, Nucl. Instrum. Methods Phys. Res. B **100**, 272 (1995).
[13] K. Kimura, J. P. Gibbons, S. B. Elston, C. Biedermann, R. DeSerio, N. Keller, J. C. Levin, M. Breinig, J. Burgdörfer, and I. A. Sellin, Phys. Rev. Lett. **66**, 25 (1991).
[14] H. F. Krause and S. Datz, Adv. At., Mol., Opt. Phys. **37**, 139 (1996).
[15] T. Azuma, T. Ito, K. Komaki, Y. Yamazaki, M. Sano, M. Torikoshi, A. Kitagawa, E. Takada, and T. Murakami, Phys. Rev. Lett. **83**, 528 (1999).
[16] E. Kupfer, H. Gabriel, and J. Burgdörfer, Z. Phys. A **300**, 35 (1981).
[17] J. Burgdörfer, H. Gabriel, and E. Kupfer, Nucl. Instrum. Methods Phys. Res. **194**, 337 (1982).
[18] K. Kimura, M. Hasegawa, Y. Fujii, Y. Susuki, and M. Mannami, in *Ion Beam Interactions With Solids*, edited by F. Fujimoto (North-Holland, Amsterdam, 1988), p. 257.
[19] K. Kimura, H. Ida, M. Fritz, and M. Mannami, Phys. Rev. Lett. **76**, 3850 (1996).
[20] N. Hatke, M. Dirska, M. Grether, E. Luderer, A. Robin, A. Närmann, and W. Heiland, Phys. Rev. Lett. **79**, 3395 (1997).
[21] F. J. Garcia de Abajo, V. H. Ponce, and P. M. Echenique, Phys. Rev. Lett. **69**, 2364 (1992).
[22] F. J. Garcia de Abajo and J. M. Pitarke, Nucl. Instrum. Methods Phys. Res. B **90**, 222 (1994).
[23] F. J. Garcia de Abajo, Nucl. Instrum. Methods Phys. Res. B **125**, 1 (1997).
[24] C. Auth, A. Mertens, H. Winter, A. G. Borisov, and G. F. Garcia de Abajo, Phys. Rev. Lett. **79**, 4477 (1997).

[25] D. S. Gemmell, Rev. Mod. Phys. **46**, 129 (1974).
[26] F. Fujimoto, K. Komaki, A. Ootuka, E. Vilalta, Y. Iwata, Y. Hirao, T. Hasegawa, M. Sekiguchi, A. Mizobuchi, T. Hattori, and K. Kimura, Nucl. Instrum. Methods Phys. Res. B **33**, 354 (1988).
[27] P. Varga and U. Diebold, in *Low Energy Ion-Surface Interactions*, edited by J. W. Rabalais (Wiley, New York, 1994), p. 355.
[28] H. Winter, Prog. Surf. Sci. **63**, 177 (2000).
[29] K. Kimura, M. Hasegawa, and M. Mannami, Phys. Rev. B **36**, 7 (1987).
[30] Y. Fujii, S. Fujiwara, K. Narumi, K. Kimura, and M. Mannami, Surf. Sci. **277**, 164 (1992).
[31] J. F. Ziegler, J. P. Biersack, and U. Littmark, *The Stopping and Range of Ions in Solids* (Pergamon, New York, 1985).
[32] H. Winter, J. Phys.: Condens. Matter **8**, 10 149 (1996).
[33] A. G. Borisov (unpublished).
[34] H. Winter, C. Auth, and A. Mertens, Nucl. Instrum. Methods Phys. Res. B (to be published).
[35] H. Winter, Z. Phys. D: At., Mol. Clusters **17**, 109 (1990).
[36] J. N. M. van Wunnik, R. Brako, K. Makoshi, and D. M. Newns, Surf. Sci. **261**, 618 (1983).
[37] J. Los and J. J. C. Geerlings, Phys. Rep. **190**, 133 (1990).
[38] T. Hecht and H. Winter, Phys. Lett. A **243**, 306 (1998).
[39] H. Winter and H. W. Ortjohann, Rev. Sci. Instrum. **58**, 359 (1987).
[40] I. Martinson and A. Gaupp, Phys. Rep., Phys. Lett. **15C**, 113 (1974).
[41] R. Krotkov and J. Stone, Phys. Rev. A **22**, 473 (1980).